Patulignans A−C, three structurally unique lignans from the leaves of *Melicope patulinervia*

Van-Tuan Vu,[a] Manh-Tuyen Nguyen,[b] Wen-Li Wang,[a] Bich-Ngoc Nguyen,[b] Giang-Nam Pham,[c] Ling-Yi Kong*[a] and Jian-Guang Luo*[a]

[a] *Jiangsu Key Laboratory of Bioactive Natural Product Research and State Key Laboratory of Natural Medicines, School of Traditional Chinese Pharmacy, China Pharmaceutical University, Nanjing 210009, People's Republic of China*

[b]*Department of Traditional Medicine, Hanoi University of Pharmacy, 13-15 Le Thanh Tong, Hoan Kiem, Hanoi, Vietnam*

[c] *College of Pharmacy, Chungnam National University, Daejeon, Republic of Korea*

Corresponding authors

* Ling-Yi Kong:

E-mail: cpu_lykong@126.com

Tel/Fax: +86-25-8327-1405

* Jian-Guang Luo:

E-mail: luojg@cpu.edu.cn

Tel/Fax: +86-25-8327-1405

Table of Contents

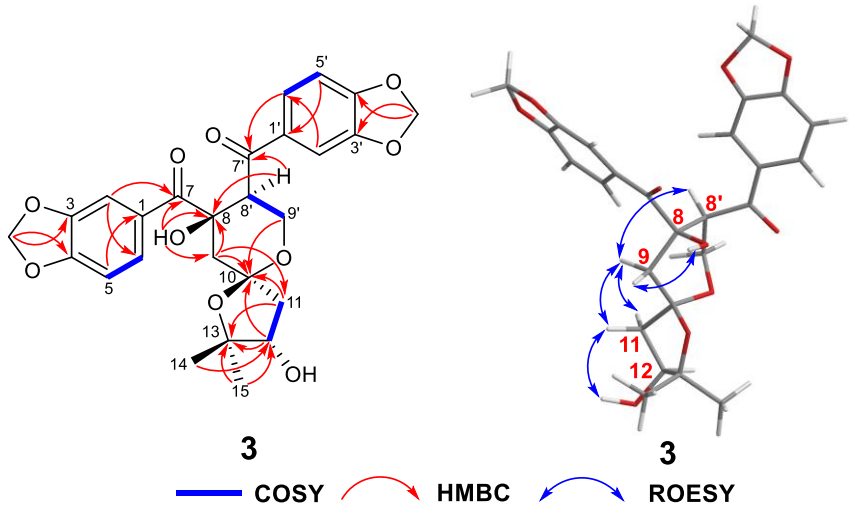

Fig. S1. COSY and key HMBC, ROESY correlations of compound **3**

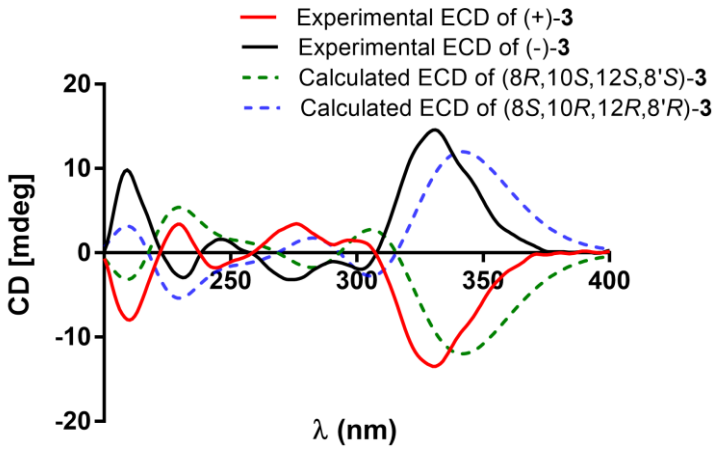

Fig. S2. Calculated and experimental ECD spectra of **3**

Table S1 Inhibitory activity against α-glucosidase of isolated compounds

No	Compounds	α-Glucosidase inhibition (IC_{50})[a]
1	(±)-Patulignan A (**1**)	5.44 ± 0.67 μM
2	(+)-Patulignan A (**1**)	6.28 ± 0.46 μM
3	(−)-Patulignan A (**1**)	8.22 ± 0.34 μM
4	(±)-Patulignan B (**2**)	32.17 ± 2.16 μM
5	(+)-Patulignan B (**2**)	34.08 ± 4.02 μM
6	(−)-Patulignan B (**2**)	30.55 ± 2.99 μM
7	(±)-Patulignan C (**3**)	52.06 ± 3.85 μM
8	(+)-Patulignan C (**3**)	47.44 ± 4.82 μM
9	(−)-Patulignan C (**3**)	50.08 ± 3.18 μM
10	Acarbose[b]	106.72 ± 8.10 μM

[a]The values indicate 50% inhibitory effects. These data represent the average values of three repeated experiments.

[b]Acarbose was used as the positive control (IC_{50} value of acarbose in reference[1] as 125.86 ± 4.12 μM).

1. Experimental section

1.1. General experimental procedures

Optical rotations were recorded on a JASCO P-1020 polarimeter in MeOH at room temperature. UV spectra were performed on a UV−2450 spectrophotometer. IR spectra were recorded in KBr disc on a Bruker Tensor 27 spectrometer. A JASCO J–810 spectropolarimeter (Jasco, Tokyo, Japan) was used to collect electronic circular dichroism (ECD) spectra. Nuclear magnetic resonance (NMR) spectra were recorded on a Bruker AVIII-600 NMR and a Bruker AVIII-500 NMR instruments equipped with CryoProbe (Bruker, Karlsruhe, Germany). High-resolution electrospray ionization (HRESIMS) spectra were measured on an Agilent 6529B Q-TOF instrument (Agilent Technologies, Santa Clara, CA, USA). Preparative HPLC was carried out on a Shimadzu LC-6A system (Shimadzu, Tokyo, Japan) equipped with a Shim-pack RP-C_{18} column (200 × 20 mm; 10 μm). Preparative chiral HPLC was performed on a Shimadzu LC-6A system with the Phenomenex column (250 mm × 21.2 mm; 5 μm).

1.2. Plant material

The leaves of *Melicope patulinervia* were collected from Hainan Province, People's Republic of China, in August 2017, and authenticated by Prof. Minjian Qin of the Research Department of Pharmacognosy, China Pharmaceutical University. A voucher specimen was deposited in the Department of Natural Medicinal Chemistry, China Pharmaceutical University (accession number 2017-MPL).

1.3. Extraction and isolation

The dried leaves of *M. patulinervia* (1.5 kg) were extracted using 95% aqueous EtOH (5 L × 3 times × 4 hours at room temperature) with ultrasonic assistance. The combined extracts were filtered and evaporated under reduced pressure to yield a green residue (172.6 g). The crude extract was suspended in distilled H_2O (2 L) and successively partitioned with CH_2Cl_2 and EtOAc. The CH_2Cl_2 extract (54.8 g) was initially fractionated by normal-phase silica gel

chromatography column (CC) eluted with a gradient of petroleum ether−ethyl acetate (1:0, 10:1, 4:1, 2:1, 1:1 *v*/*v*) to give six fractions (A−F). Fraction C (9.6 g) was chromatographed on an ODS CC eluted with a gradient system of MeOH−H_2O (3:2, 4:1, 9:1, 9.5:1, 1:0, *v*/*v*) to give four major fractions (C1−C4). Fraction C3 (3.6 g) was separated by an ODS CC (MeOH−H_2O, 4:1 to 5:1, *v*/*v*) to obtain six sub-fractions (C3.1−C3.6). Subfraction C3.2 was purified using preparative RP-HPLC (MeOH−H_2O, 60:40, 65:35 *v*/*v*) to yield **1** (9 mg), **2** (13 mg), and **3** (12 mg). Subsequently, enantiomers (+)-**1** (1.8 mg), (−)-**1** (1.8 mg), (+)-**2** (2.2 mg), (−)-**2** (2.0 mg), (+)-**3** (2.1 mg), and (−)-**3** (2.1 mg), respectively were obtained from corresponding racemates by the preparative chiral HPLC using the Phenomenex chiral column with MeOH-H_2O (85/15; 90/10, *v*/*v*) as the mobile phase.

1.4. *α*-glucosidase inhibitory assay

The *α*-glucosidase inhibitory assay was performed according to a published method with slight modification.[1] 3 mM *p*-nitrophenyl-*α*-D-glucopyranoside (20 μL) and 0.2 U/mL *α*-glucosidase (20 μL) in 0.01 M phosphate buffer (pH = 7.0) were added to the sample solution dissolved in DMSO (10 μL) to start the reaction. Each reaction was carried out at 37°C for 30 min and stopped by adding 0.1 M Na_2CO_3 (150 μL). The absorbance was recorded at 410 nm. All the samples were tested in triplicate, and the IC_{50} values were calculated from the dose-inhibition curve plotting using six different sample concentrations. Acarbose, a known *α*-glucosidase inhibitor was used as a positive control.

2. Physical and chemical data of patulignans A−C

Patulignan A (1): white amorphous powder; UV (MeOH) λ_{max} (log ε) 204 (4.80), 231 (4.68), 279 (4.31), 313 (4.41) nm; IR (KBr)$_{vmax}$ 3461, 1668, 1491, 1441, 1250, 1030 cm^{-1}; ^1H and ^{13}C NMR data, see Table 1; HR-ESIMS *m/z*: 521.1415 $[M + Na]^+$ (calcd for $C_{26}H_{26}O_{10}Na$, 521.1418). (+)-**1**: $[\alpha]_D^{25}$ +76.2 (*c* 0.11, MeOH); ECD (MeOH) λ (Δε) 206 (−2.61), 236 (+2.00),

276 (+0.94), 328 (−3.91). (−)-**1**: $[\alpha]_D^{25}$ −75.1 (*c* 0.13, MeOH); ECD (MeOH) λ (Δε) 208 (+2.32), 236 (−2.02), 278 (−0.67), 329 (+4.18).

Patulignan B (2): white amorphous powder; UV (MeOH) λ_{max} (log ε) 205 (4.81), 232 (4.80), 280 (4.44), 315 (4.55) nm; IR (KBr)$_{\nu max}$ 3454, 2926, 1650, 1495, 1447, 1257, 1043 cm^{-1}; ^{1}H and ^{13}C NMR data, see Table 1; HR-ESIMS *m/z*: 521.1414 [M + Na]$^+$ (calcd for $C_{26}H_{26}O_{10}Na$, 521.1418). (+)-**2**: $[\alpha]_D^{25}$ +65.2 (*c* 0.10, MeOH); ECD (MeOH) λ (Δε) 209 (−6.57), 230 (+1.98), 275 (+2.30), 329 (−10.35). (−)-**2**: $[\alpha]_D^{25}$ −66.1 (*c* 0.11, MeOH); ECD (MeOH) λ (Δε) 208 (+6.85), 230 (−1.76), 273 (−1.76), 330 (+8.96).

Patulignan C (3): white amorphous powder; UV (MeOH) λ_{max} (log ε) 204 (4.80), 233 (4.79), 279 (4.44), 315 (4.54) nm; IR (KBr)$_{\nu max}$ 3442, 1657, 1493, 1387, 1250, 1112 cm^{-1}; ^{1}H and ^{13}C NMR data, see Table 1; HR-ESIMS *m/z*: 521.1416 [M + Na]$^+$ (calcd for $C_{26}H_{26}O_{10}Na$, 521.1418). (+)-**3**: $[\alpha]_D^{25}$ +61.6 (*c* 0.12, MeOH); ECD (MeOH) λ (Δε) 209 (−7.91), 230 (+3.39), 276 (+3.44), 330 (−13.47). (−)-**3**: $[\alpha]_D^{25}$ −60.3 (*c* 0.10, MeOH); ECD (MeOH) λ (Δε) 209 (+9.81), 231 (−2.94), 275 (−3.18), 331 (+14.59).

3. ECD calculation of 1−3

The 3D structures of selected compounds were subjected to Schrödinger MacroModel 9.1 (Schrödinger. LLC, USA) to perform conformational analysis using the MMFF force field in gas phase. The conformers occurring in energy window of 3 kcal/mol were chosen, and then the conformers were initially optimized at B3LYP/6-31g (d, p) level in MeOH using the CPCM polarizable conductor calculation model by Gaussian 09 program package. The theoretical calculation of ECD was conducted in MeOH using Time-dependent Density functional theory (TD-DFT) at the B3LYP/6-31g (d, p) level for all optimized stable conformers. Rotatory strengths for a total of 60 excited states were calculated. ECD spectra were generated using the program SpecDis 1.7.1 with UV correction and a half-bandwidth of σ = 0.25 eV.[2,3]

References

1. K. Chen, X. Q. Liu, W. L. Wang, J. G. Luo and L. Y. Kong, *Bioorg. Chem*., 2020, **94**, 103400.

2. M. J. Frisch, G. W. Trucks, H. B. Schlegel, G. E. Scuseria, M. A. Robb, J. R. Cheeseman, G. Scalmani, V. Barone, B. Mennucci, G. A. Petersson, H. Nakatsuji, M. Caricato, X. Li, H. P. Hratchian, A. F. Izmaylov, J. Bloino, G. Zheng, J. L. Sonnenberg, M. Hada, M. Ehara, K. Toyota, R. Fukuda, J. Hasegawa, M. Ishida, T. Nakajima, Y. Honda, O. Kitao, H. Nakai, T. Vreven, Jr. J. A. Montgomery, J. E. Peralta, F. Ogliaro, M. Bearpark, J. J. Heyd, E. Brothers, K. N. Kudin, V. N. Staroverov, T. Keith, R. Kobayashi, J. Normand, K. Raghavachari, A. Rendell, J. C. Burant, S. S. Iyengar, J. Tomasi, M. Cossi, N. Rega, J. M. Millam, M. Klene, J. E. Knox, J. B. Cross, V. Bakken, C. Adamo, J. Jaramillo, R. Gomperts, R. E. Stratmann, O. Yazyev, A. J. Austin, R. Cammi, C. Pomelli, J. W. Ochterski, R. L. Martin, K. Morokuma, V. G. Zakrzewski, G. A. Voth, P. Salvador, J. J. Dannenberg, S. Dapprich, A. D. Daniels, O. Farkas, J. B. Foresman, J. V. Ortiz, J. Cioslowski, D. J. Fox, Gaussian 09, revision C.01, Gaussian, Inc. Wallingford, CT 2009.

3. V. T. Vu, X. L. Chen, L. Y. Kong and J. G. Luo, *Org. Lett*., 2020, **22**, 1380–1384.

4. Spectra of (±)-patulignan A (1)

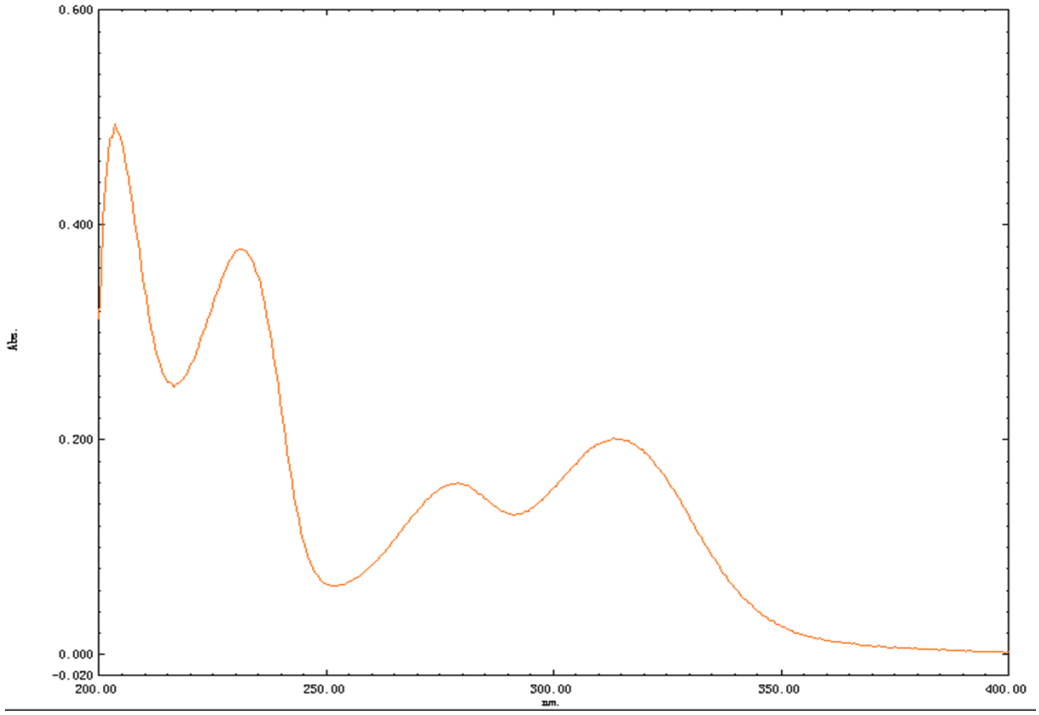

Figure S4.1. UV spectrum (MeOH) of compound **1**

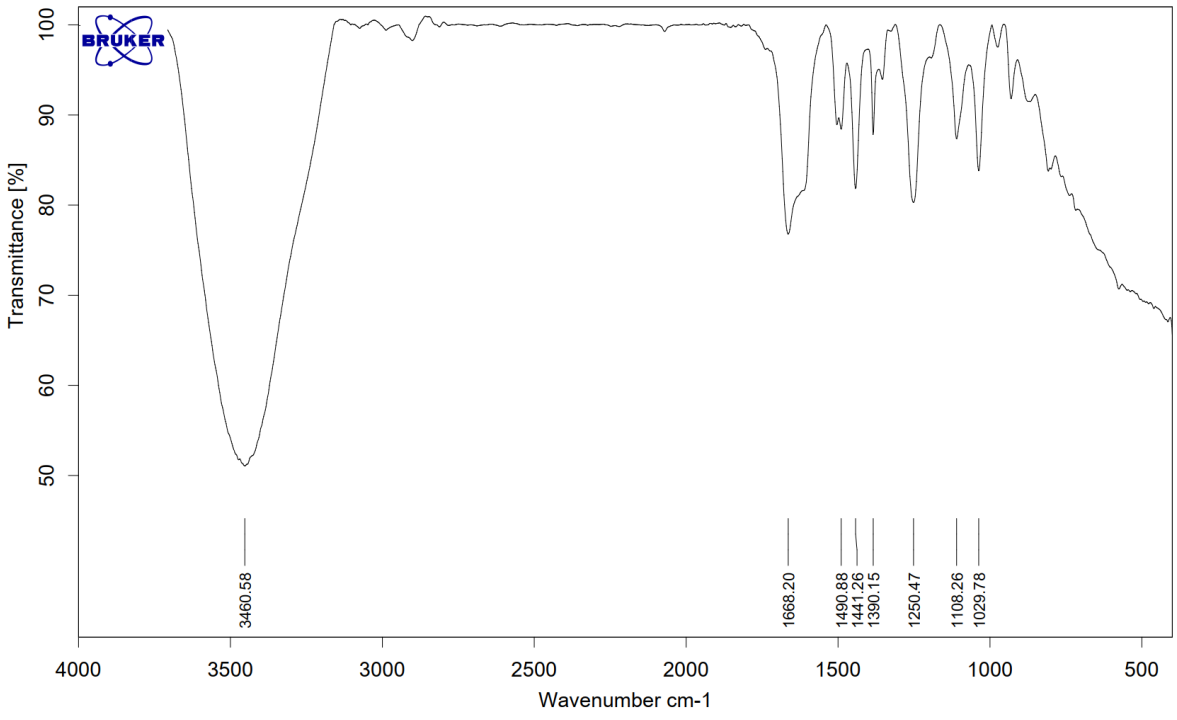

Figure S4.2. IR spectrum of compound **1**

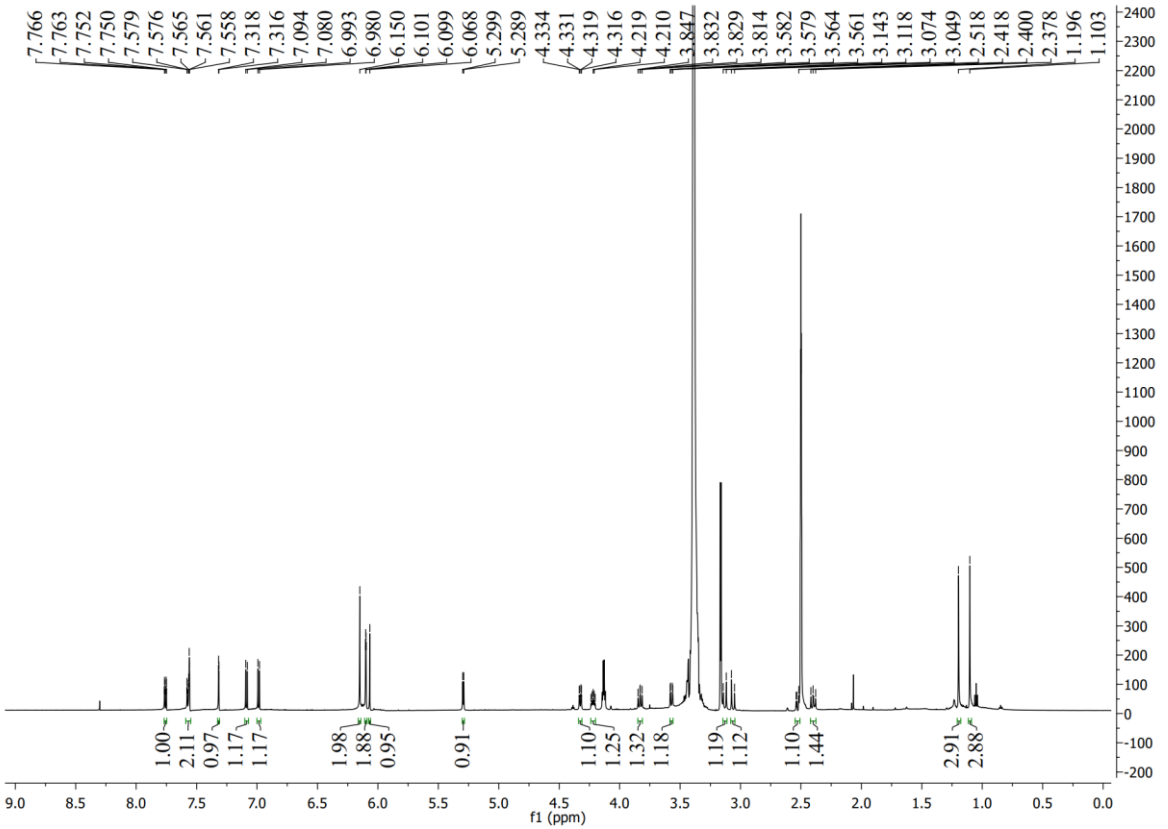

Figure S4.3. ^{1}H NMR spectrum (600 MHz, DMSO-d_6) of compound **1**

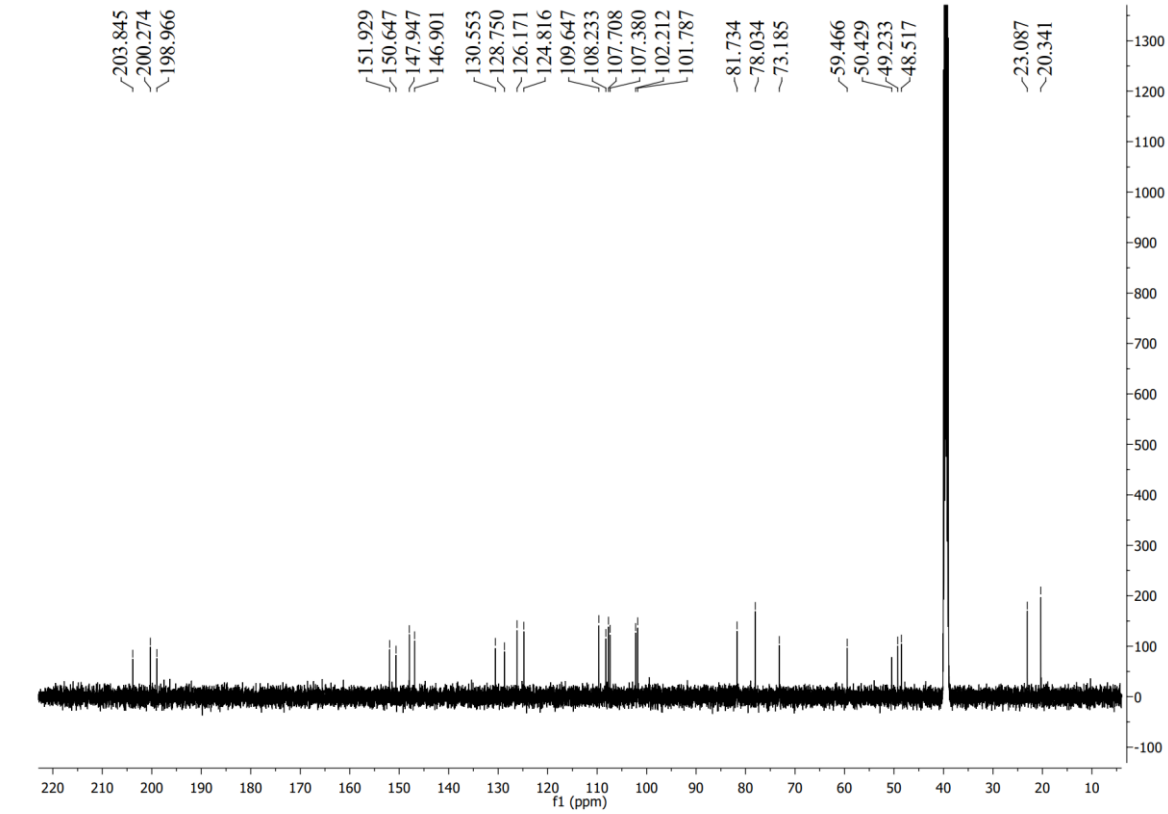

Figure S4.4. ^{13}C NMR spectrum (150 MHz, DMSO-d_6) of compound **1**

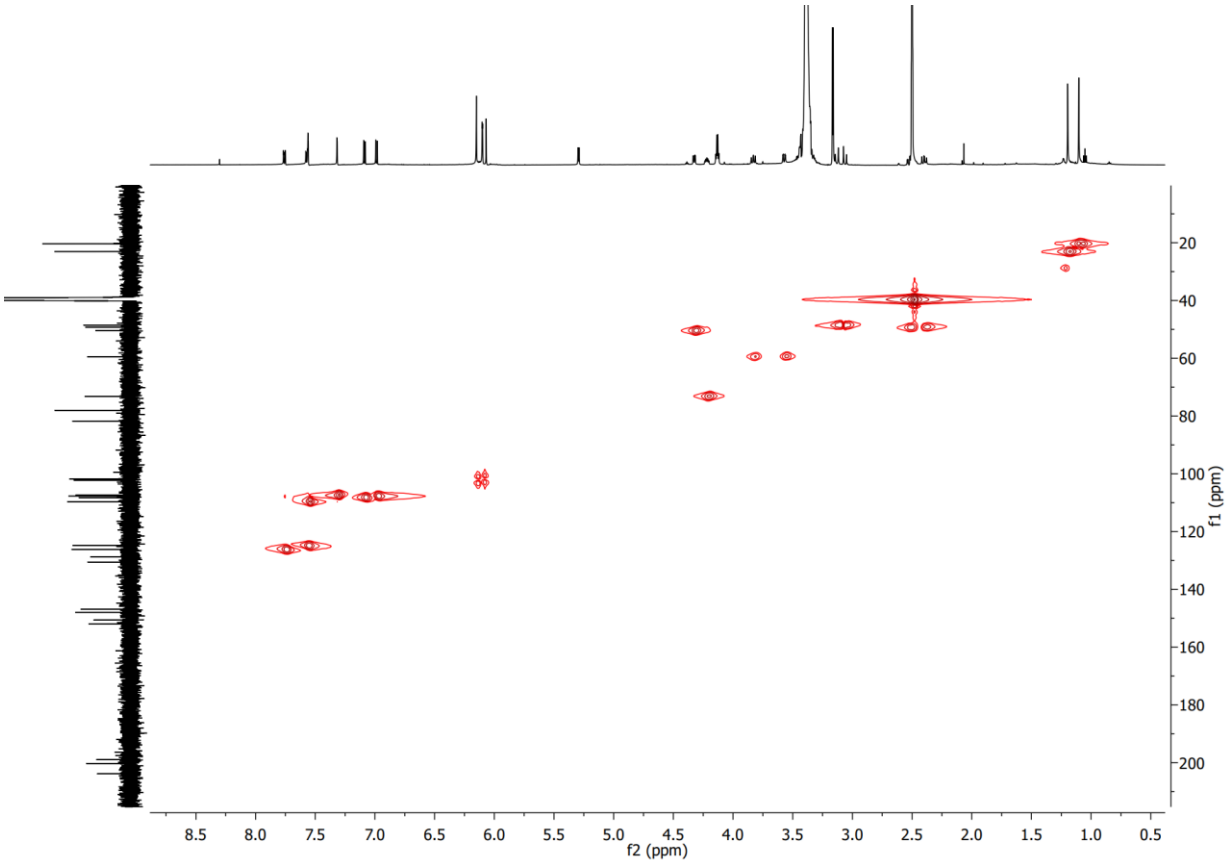

Figure S4.5. HSQC spectrum (600 MHz, DMSO-d_6) of compound **1**

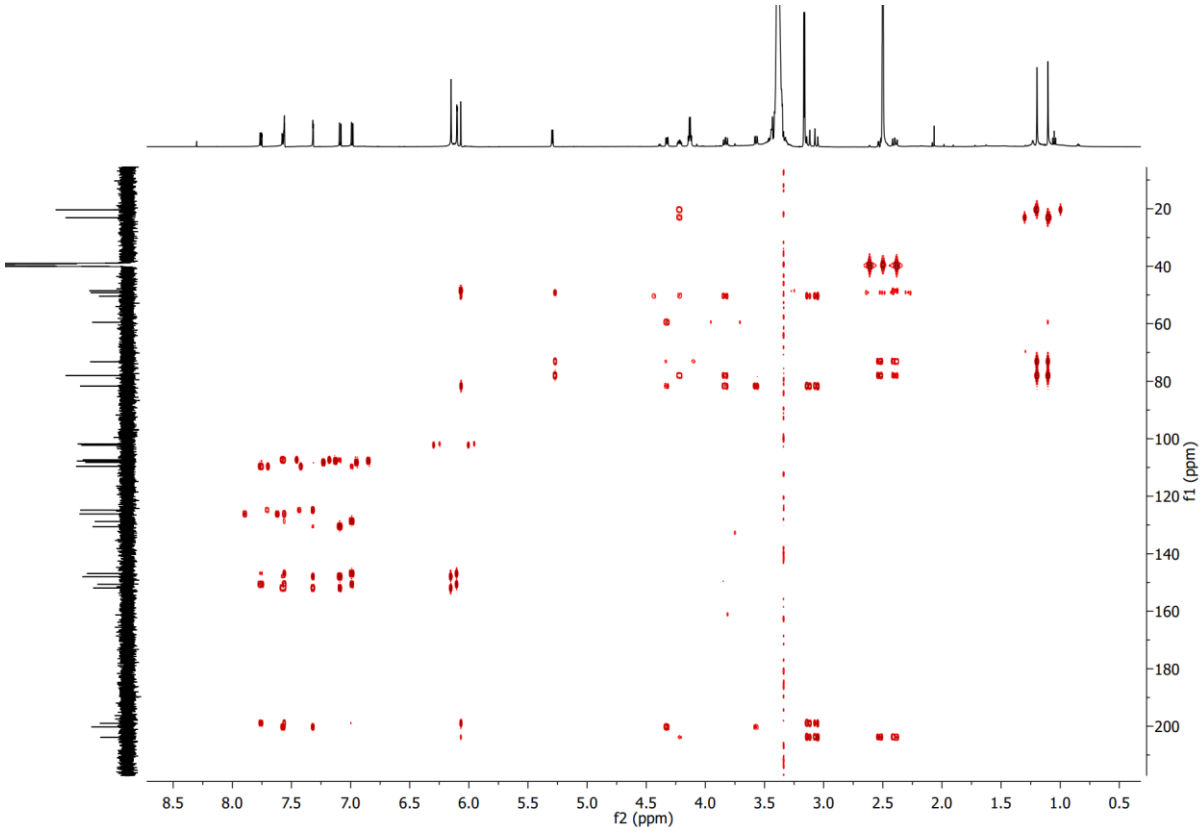

Figure S4.6. HMBC spectrum (600 MHz, DMSO-d_6) of compound **1**

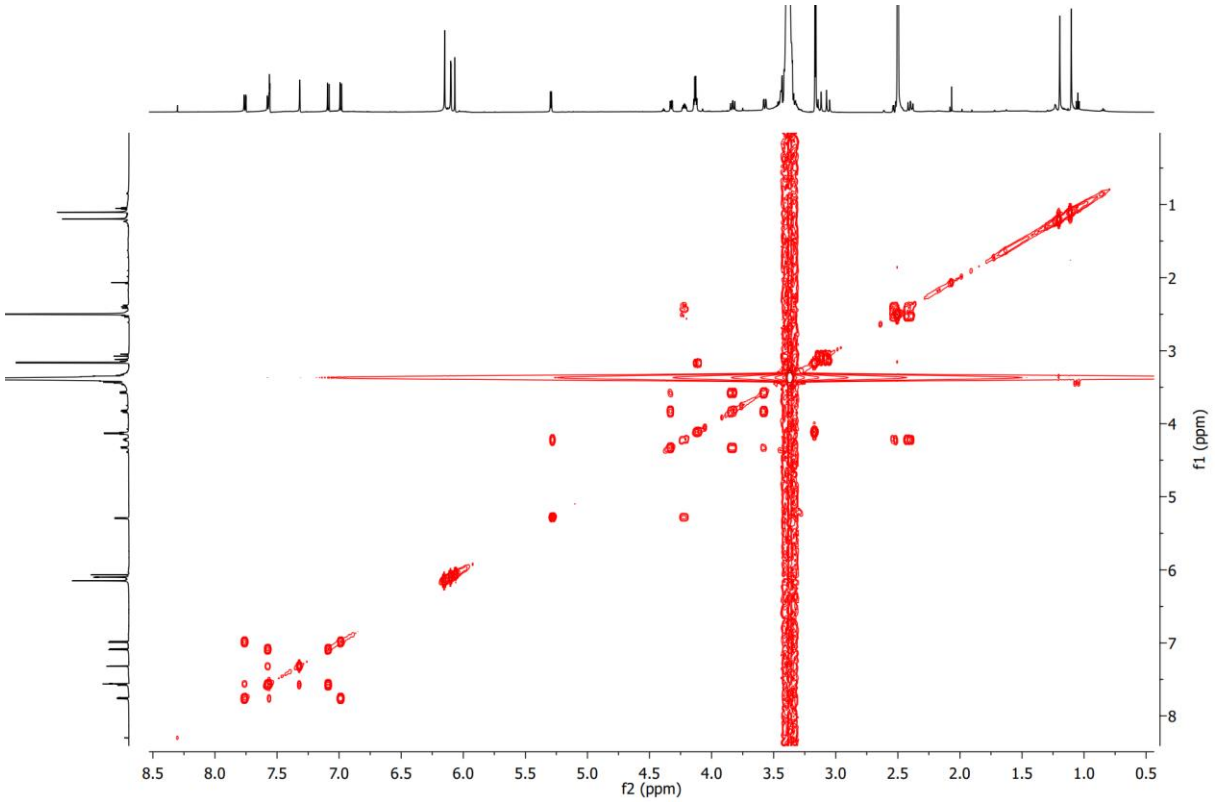

Figure S4.7. COSY spectrum (600 MHz, DMSO-d_6) of compound **1**

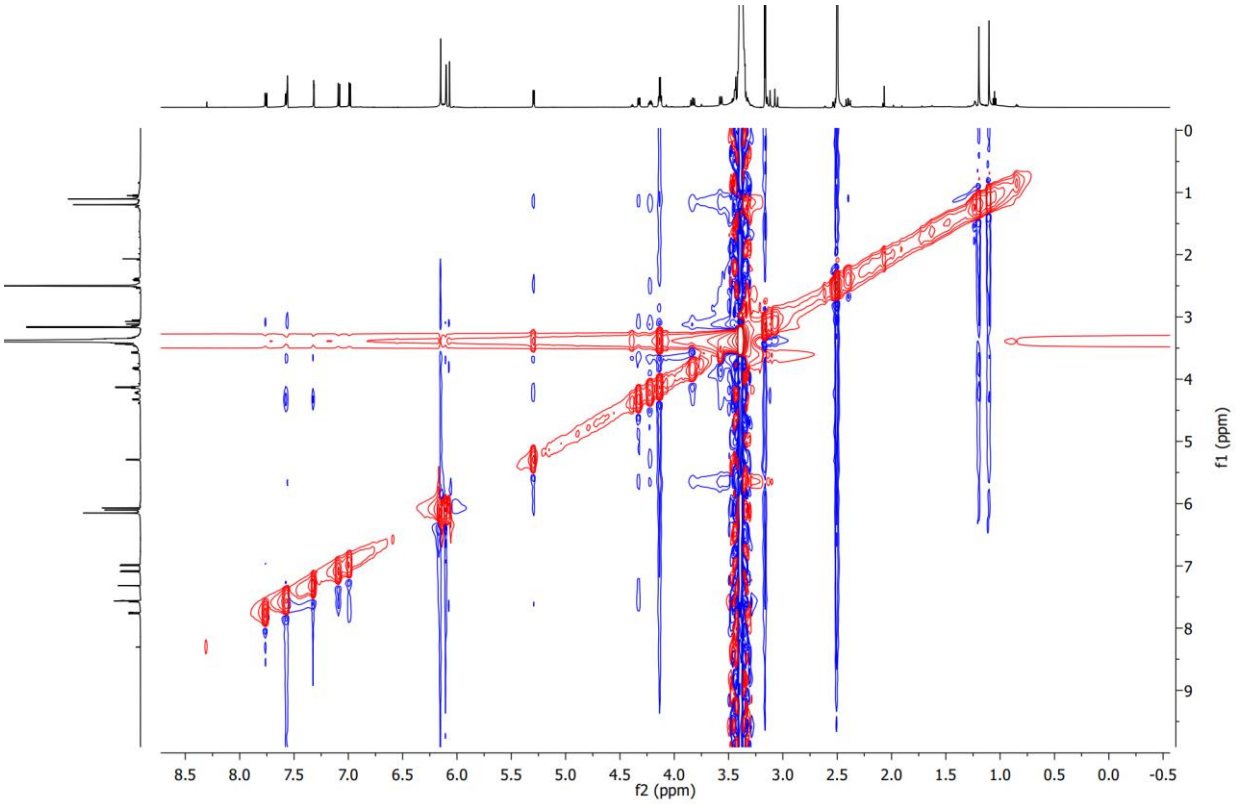

Figure S4.8. ROESY spectrum (600 MHz, DMSO-d_6) of compound **1**

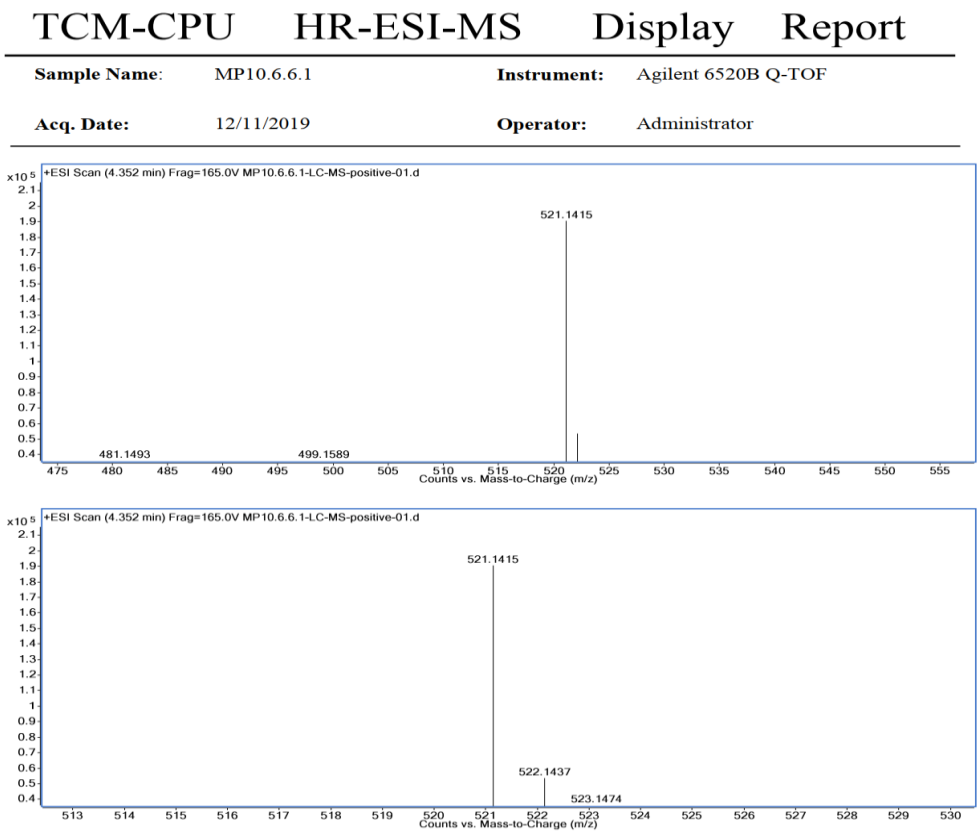

Figure S4.9. HRESIMS spectrum of compound **1**

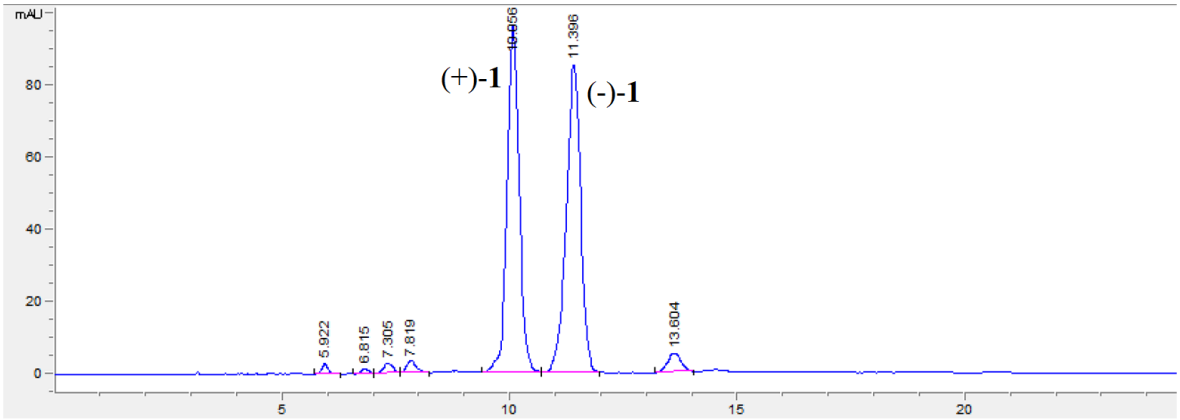

Figure S4.10. Chiral HPLC chromatogram of compound **1**

5. Spectra of (±)-patulignan B (2)

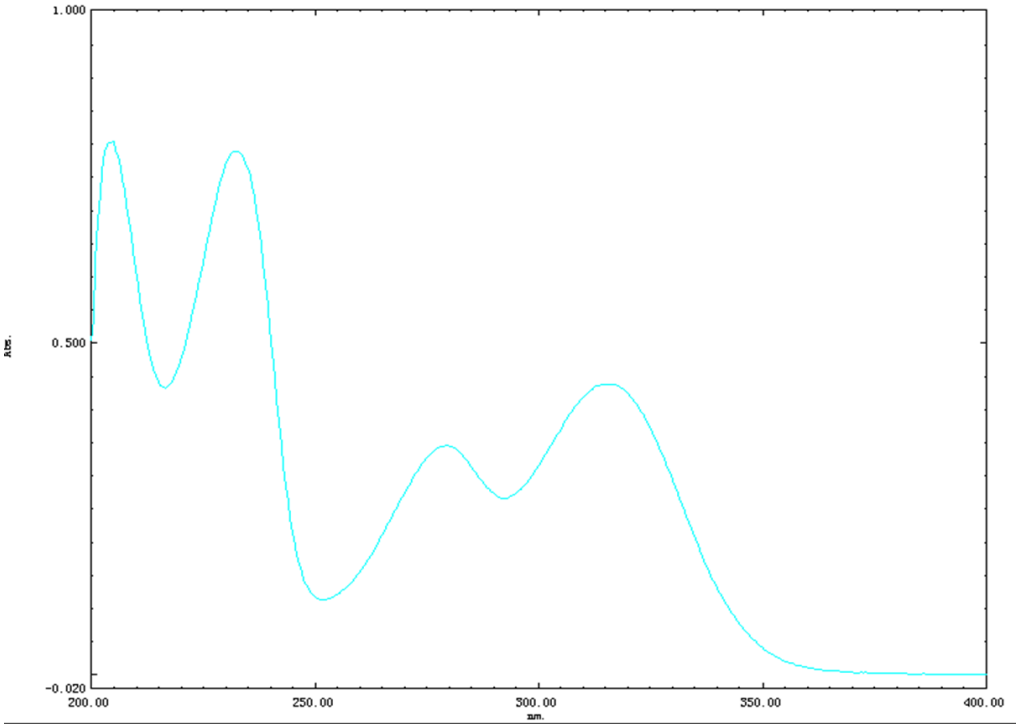

Figure S5.1. UV spectrum (MeOH) of compound **2**

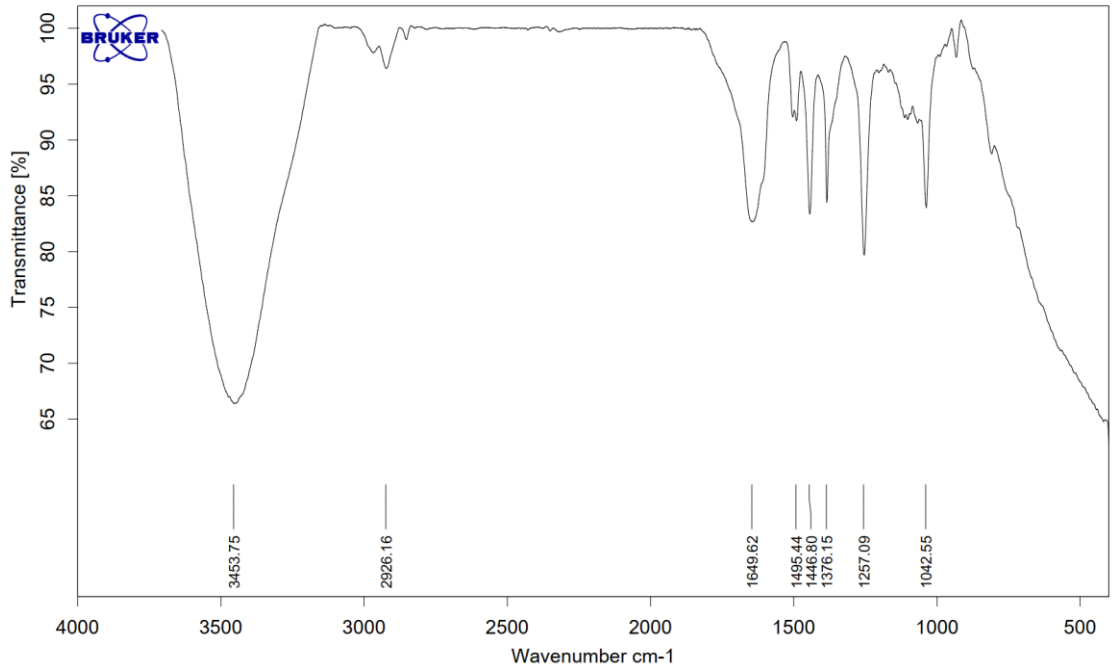

Figure S5.2. IR spectrum of compound **2**

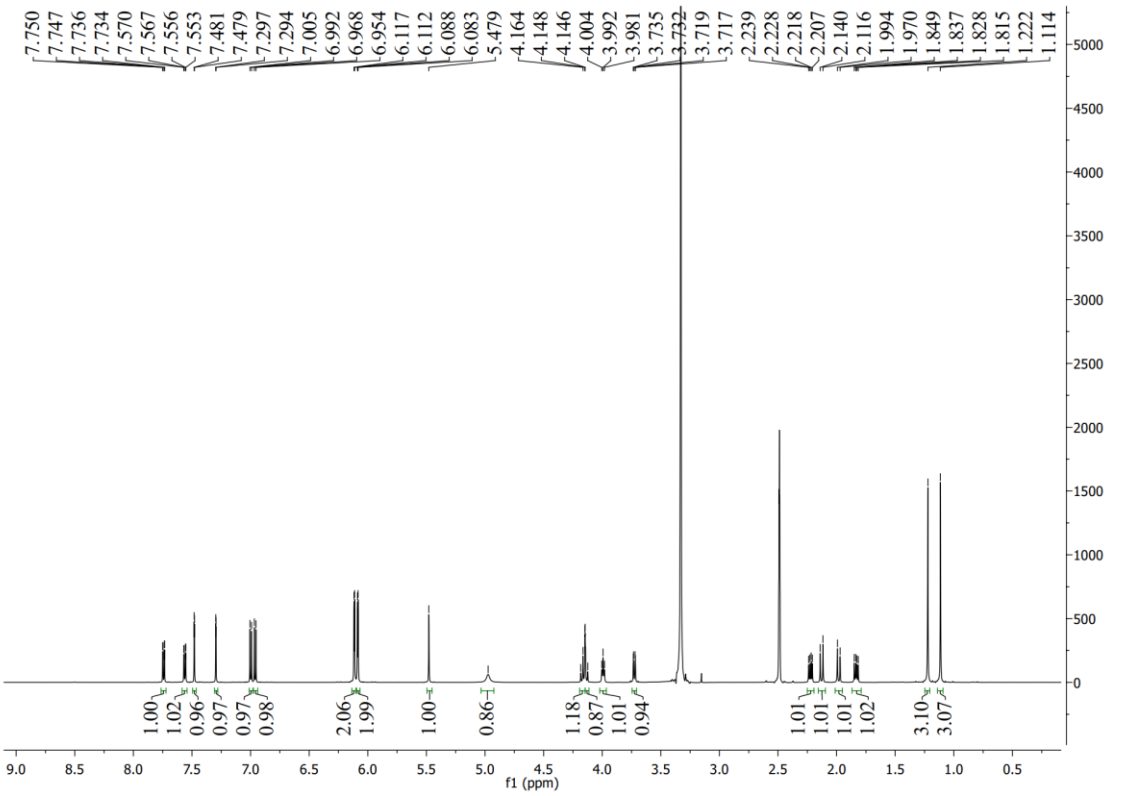

Figure S5.3. ^{1}H NMR spectrum (600 MHz, DMSO-d_6) of compound **2**

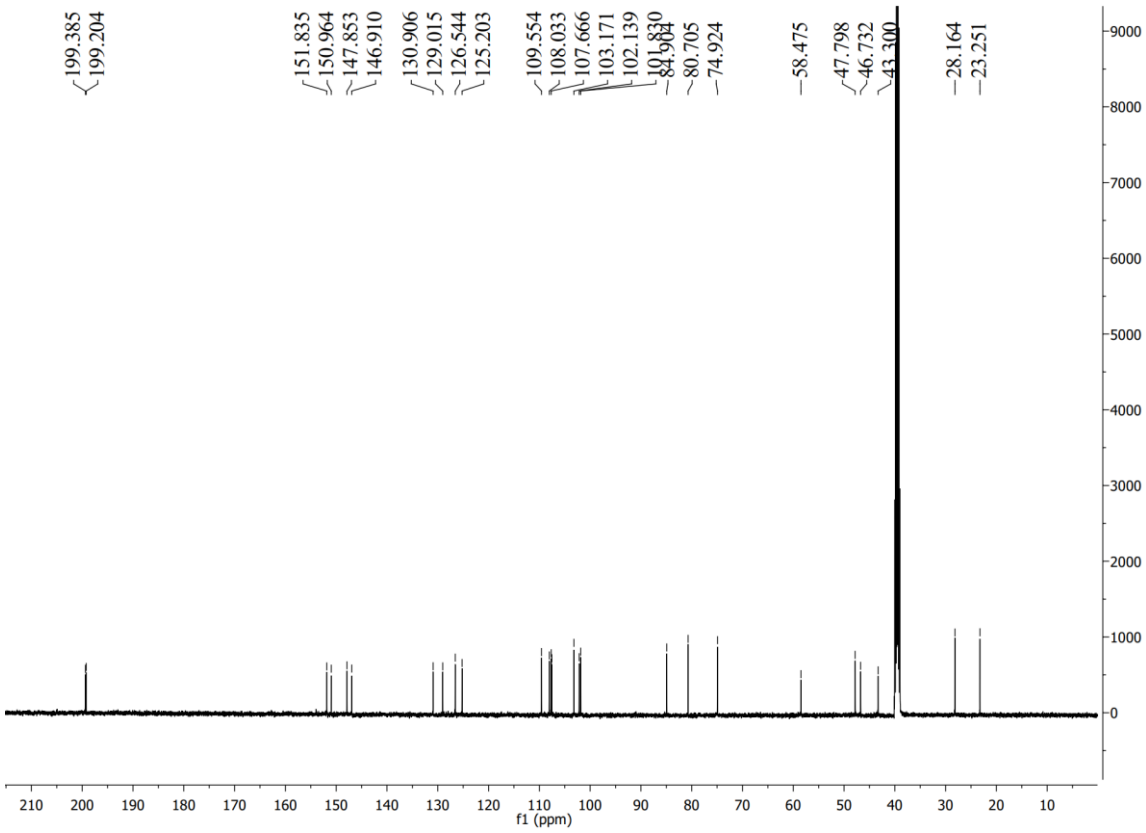

Figure S5.4. ^{13}C NMR spectrum (150 MHz, DMSO-d_6) of compound **2**

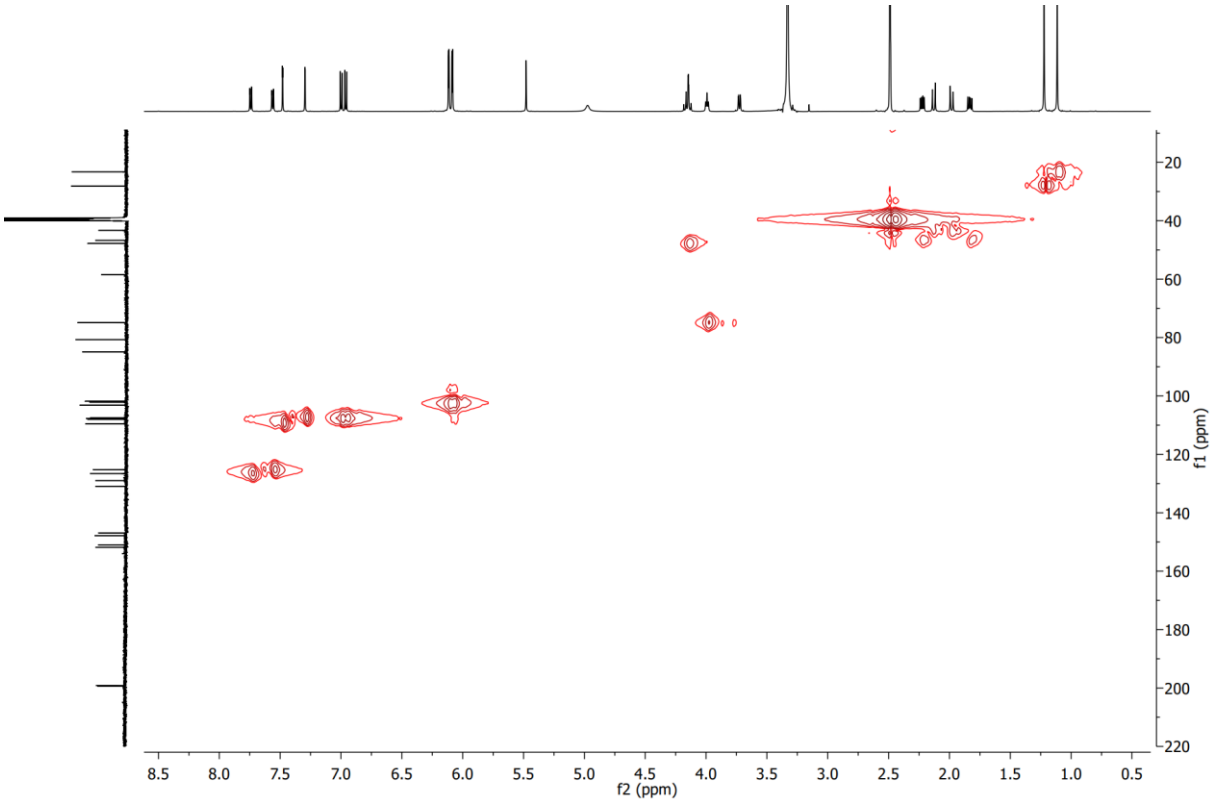

Figure S5.5. HSQC spectrum (600 MHz, DMSO-d_6) of compound **2**

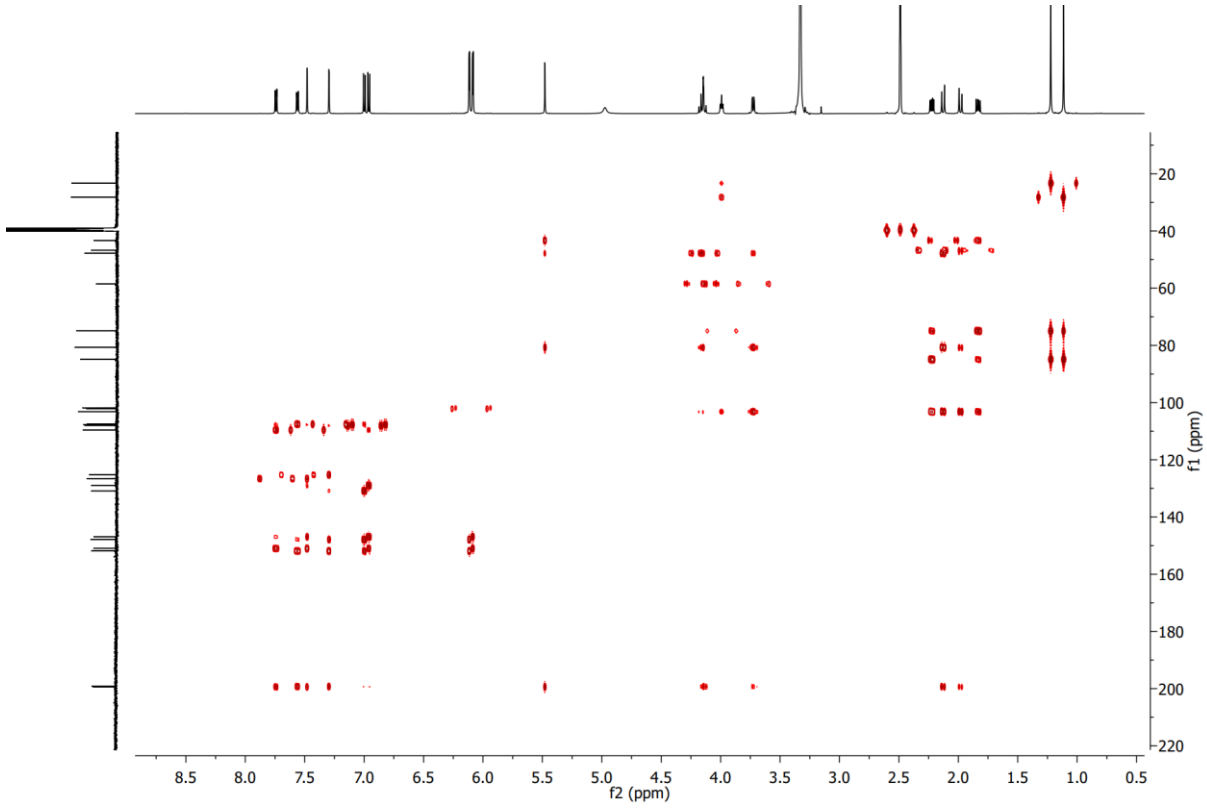

Figure S5.6. HMBC spectrum (600 MHz, DMSO-d_6) of compound **2**

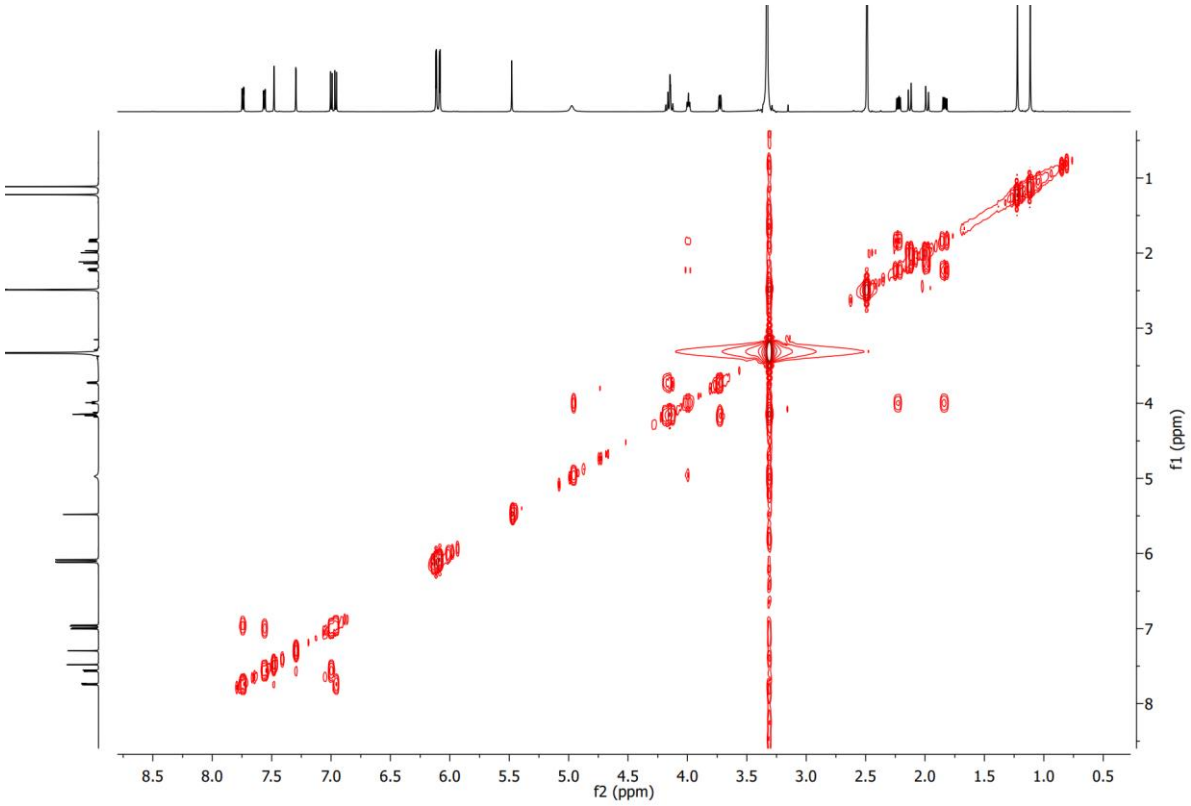

Figure S5.7. COSY spectrum (600 MHz, DMSO-d_6) of compound **2**

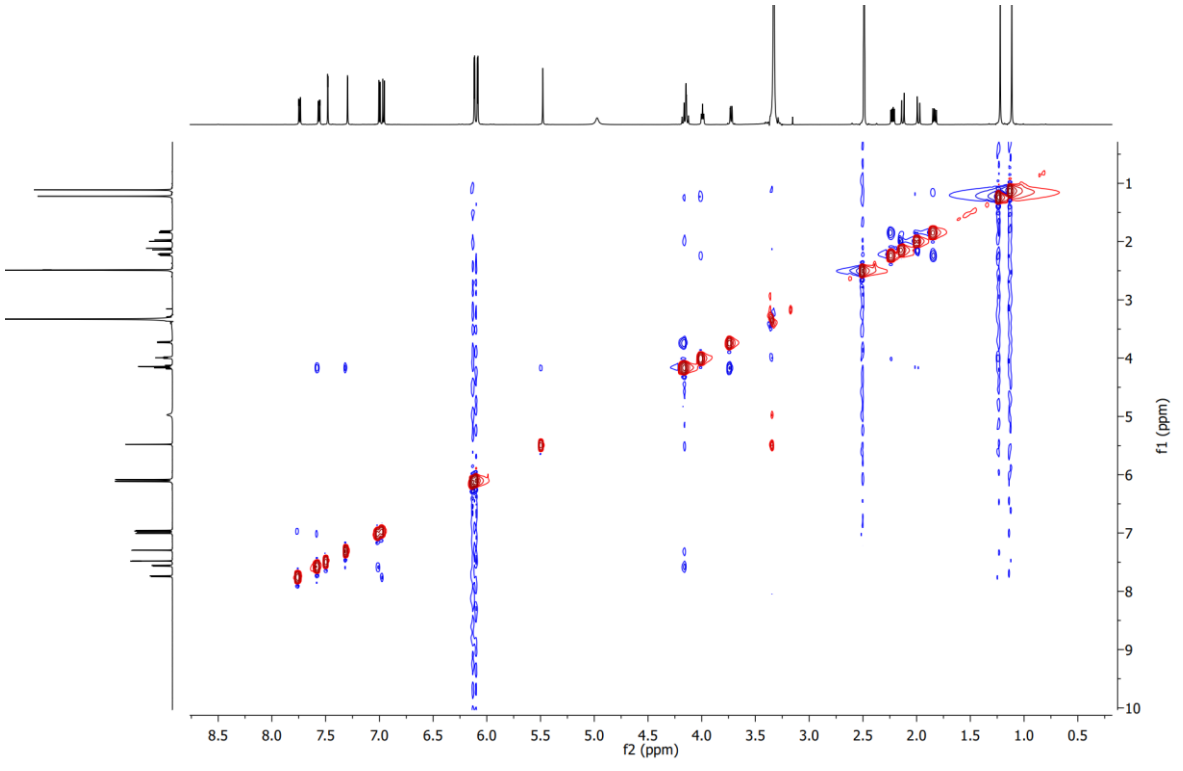

Figure S5.8. ROESY spectrum (600 MHz, DMSO-d_6) of compound **2**

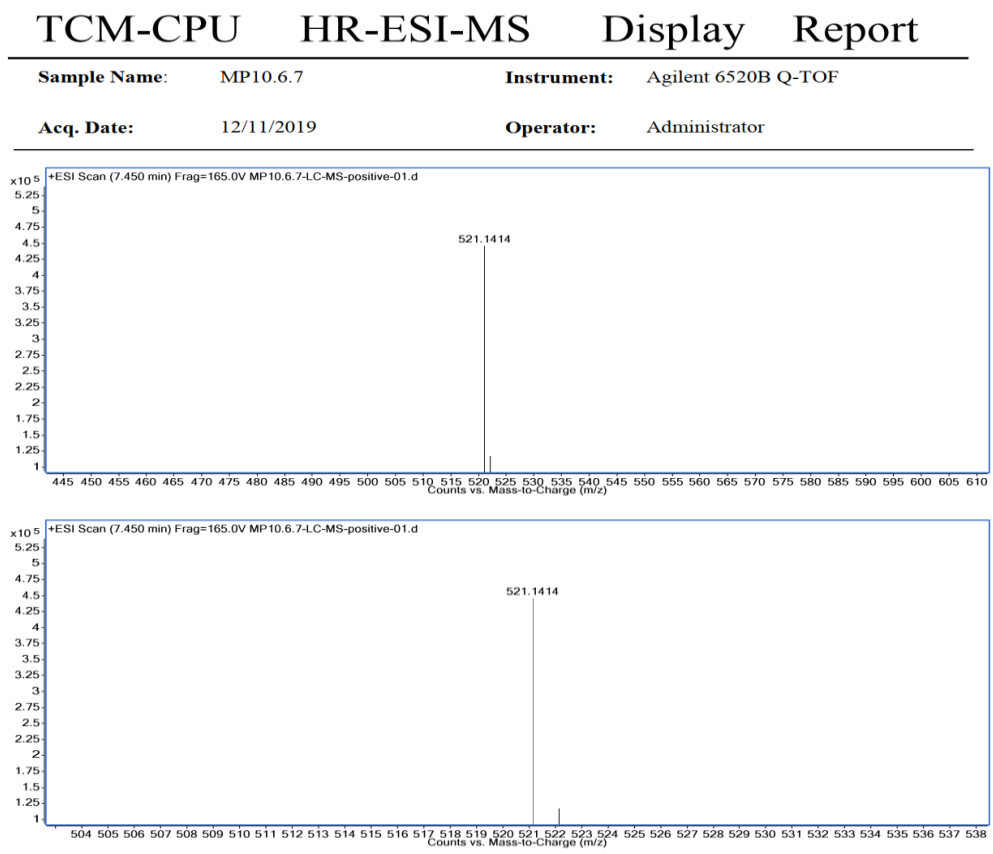

Figure S5.9. HRESIMS spectrum of compound **2**

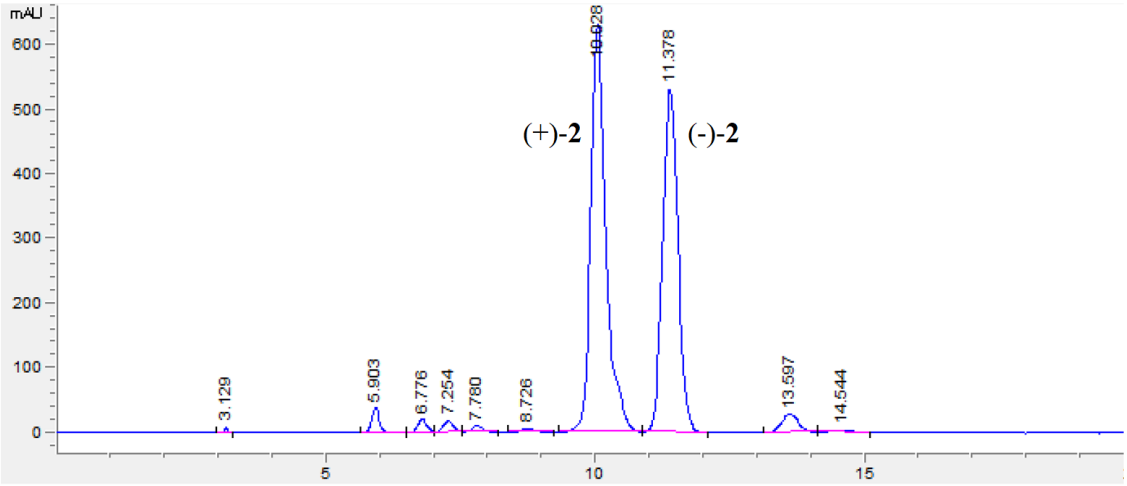

Figure S5.10. Chiral HPLC chromatogram of compound **2**

6. Spectra of (±)-patulignan C (3)

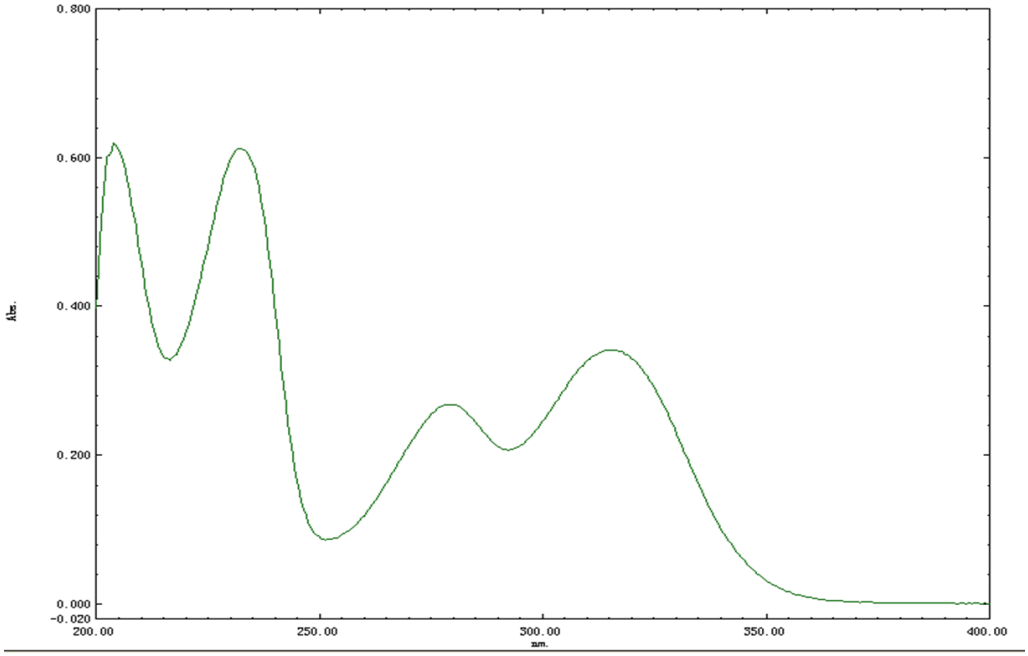

Figure S6.1. UV spectrum (MeOH) of compound **3**

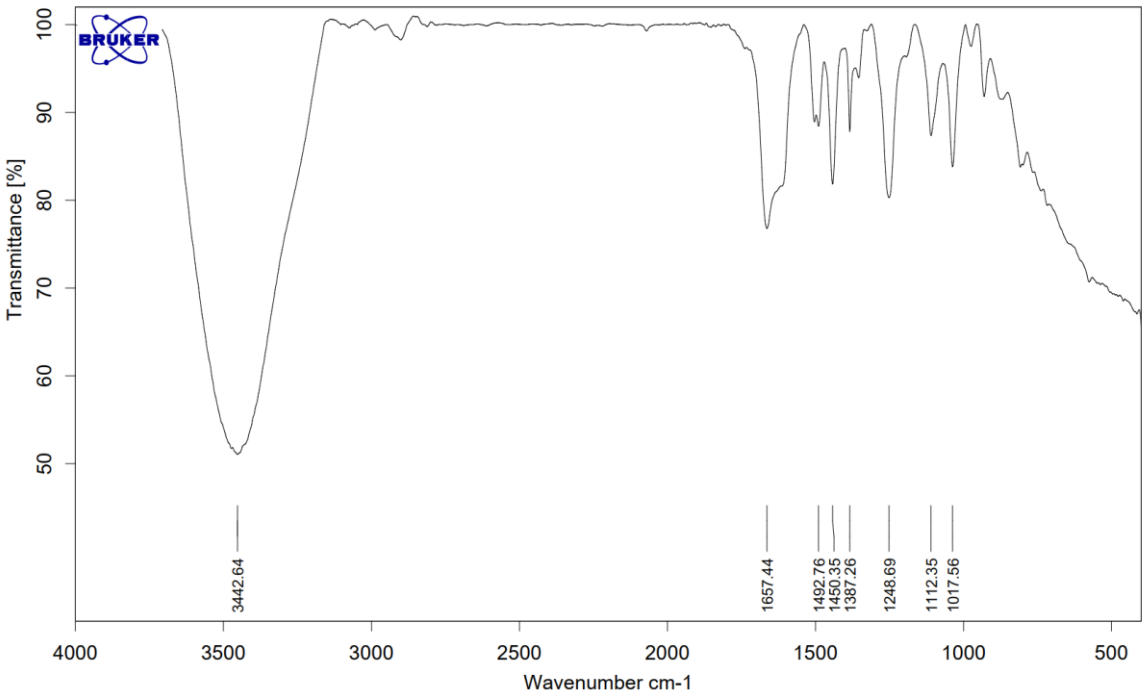

Figure S6.2. IR spectrum of compound **3**

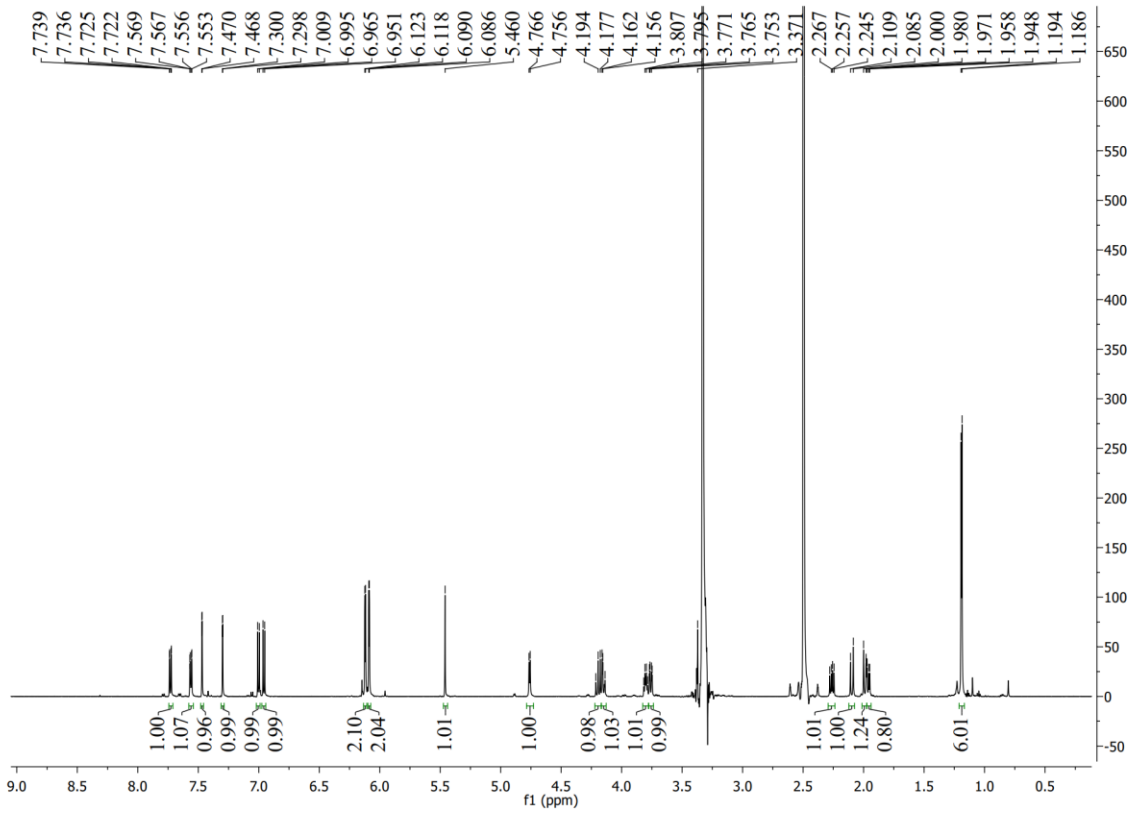

Figure S6.3. ^{1}H NMR spectrum (600 MHz, DMSO-d_6) of compound **3**

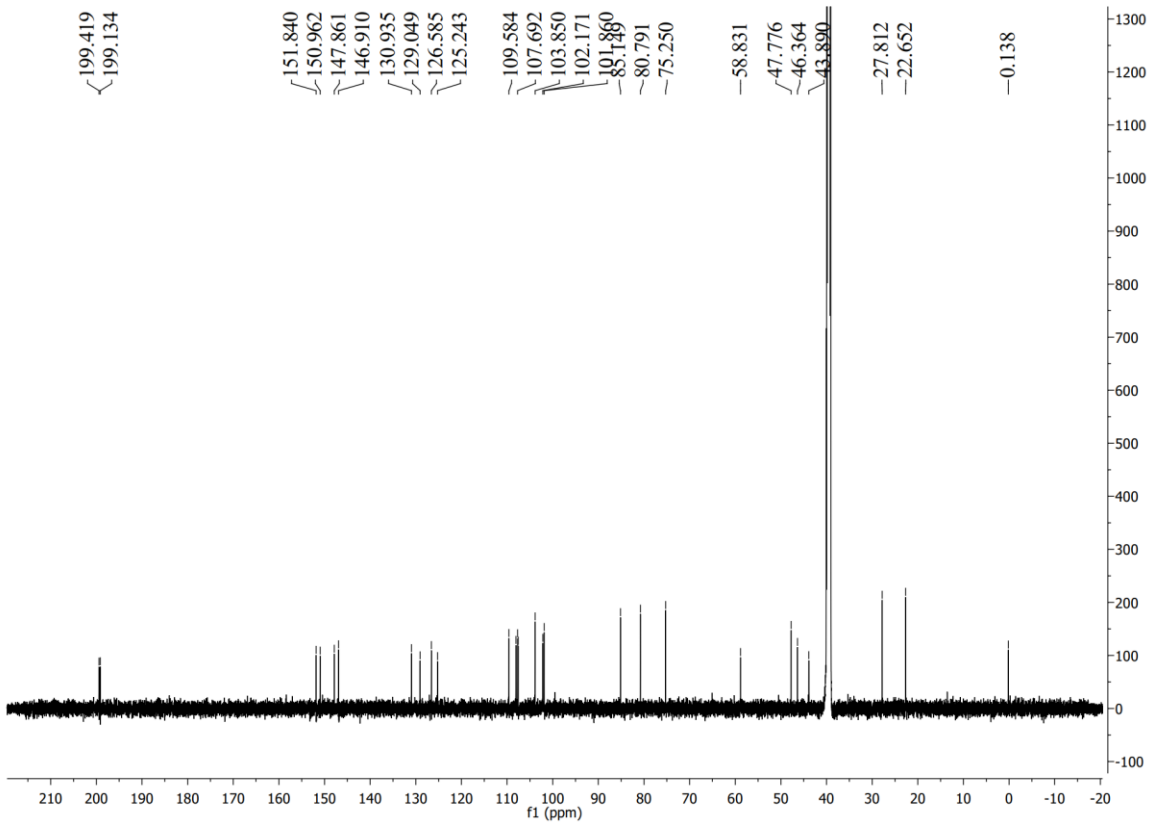

Figure S6.4. ^{13}C NMR spectrum (150 MHz, DMSO-d_6) of compound **3**

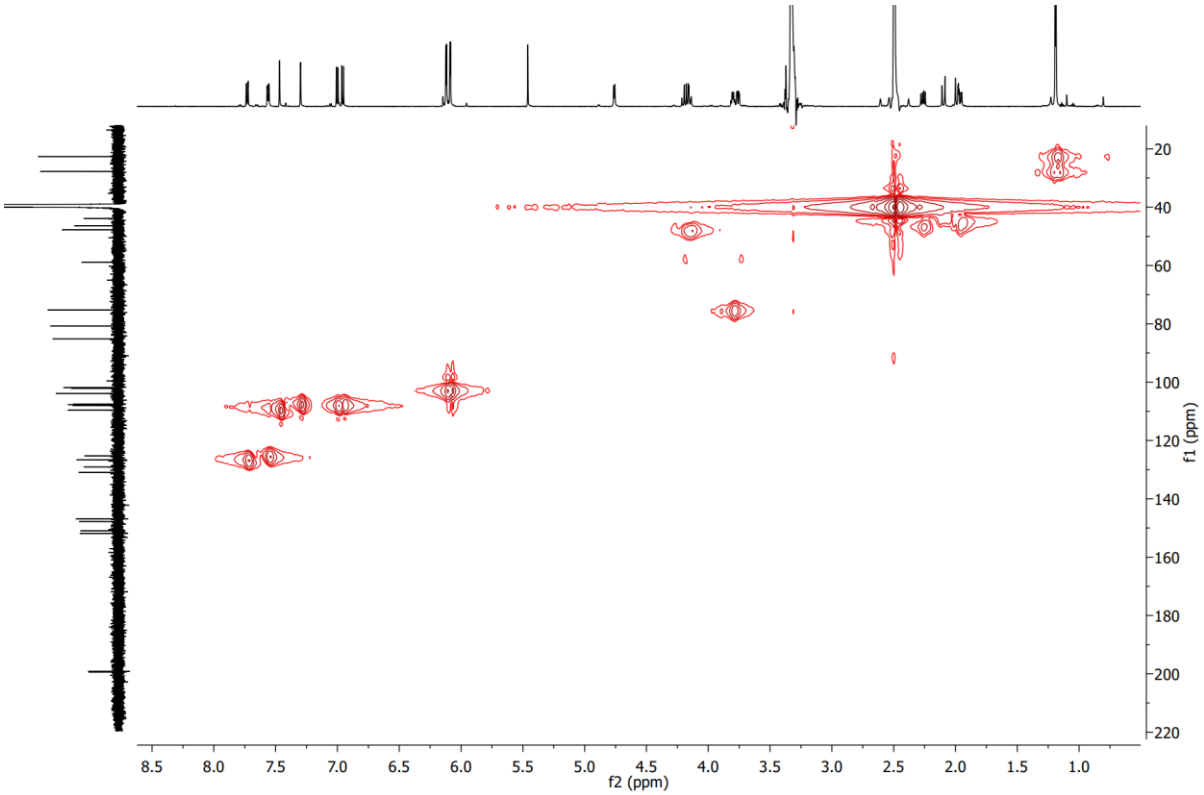

Figure S6.5. HSQC spectrum (600 MHz, DMSO-d_6) of compound **3**

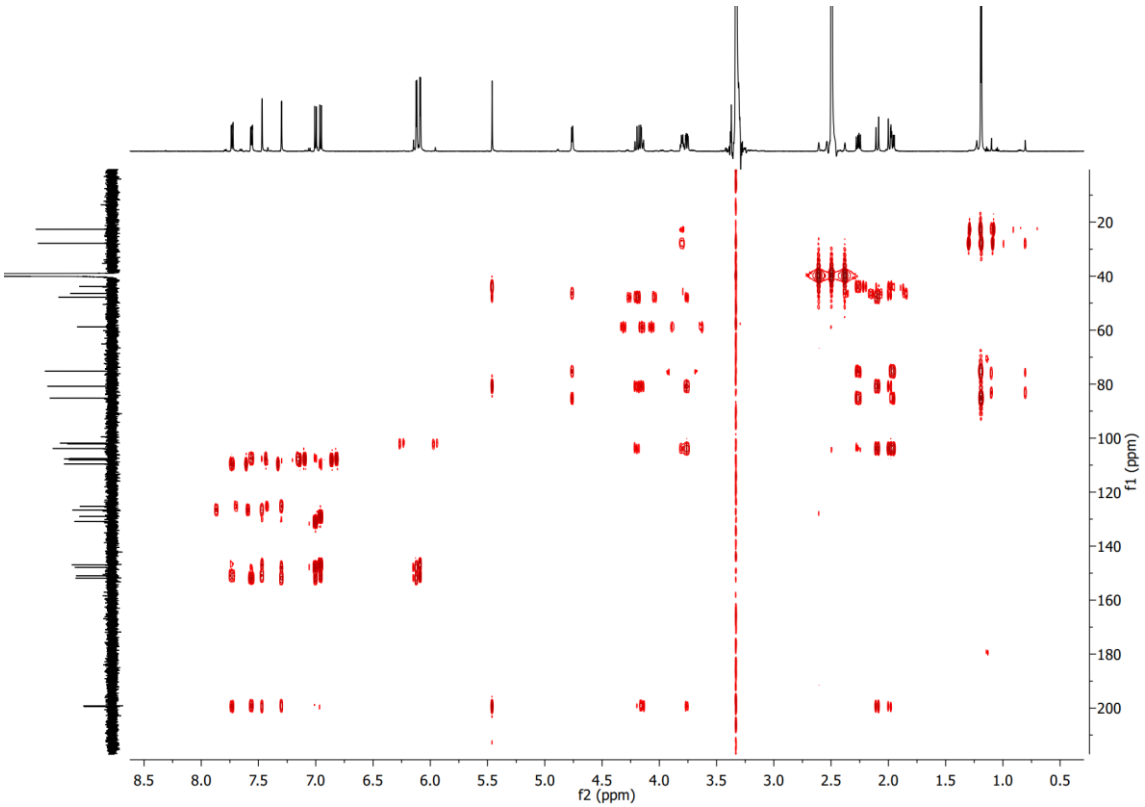

Figure S6.6. HMBC spectrum (600 MHz, DMSO-d_6) of compound **3**

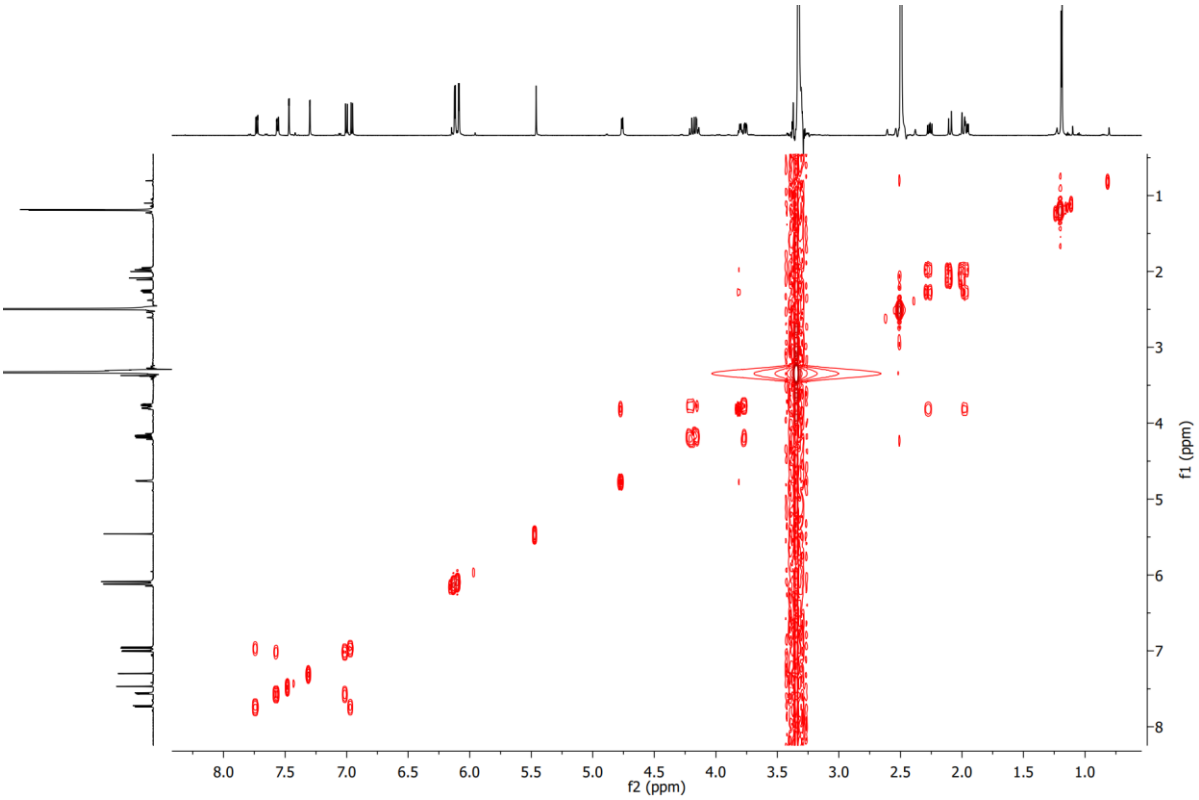

Figure S6.7. COSY spectrum (600 MHz, DMSO-d_6) of compound **3**

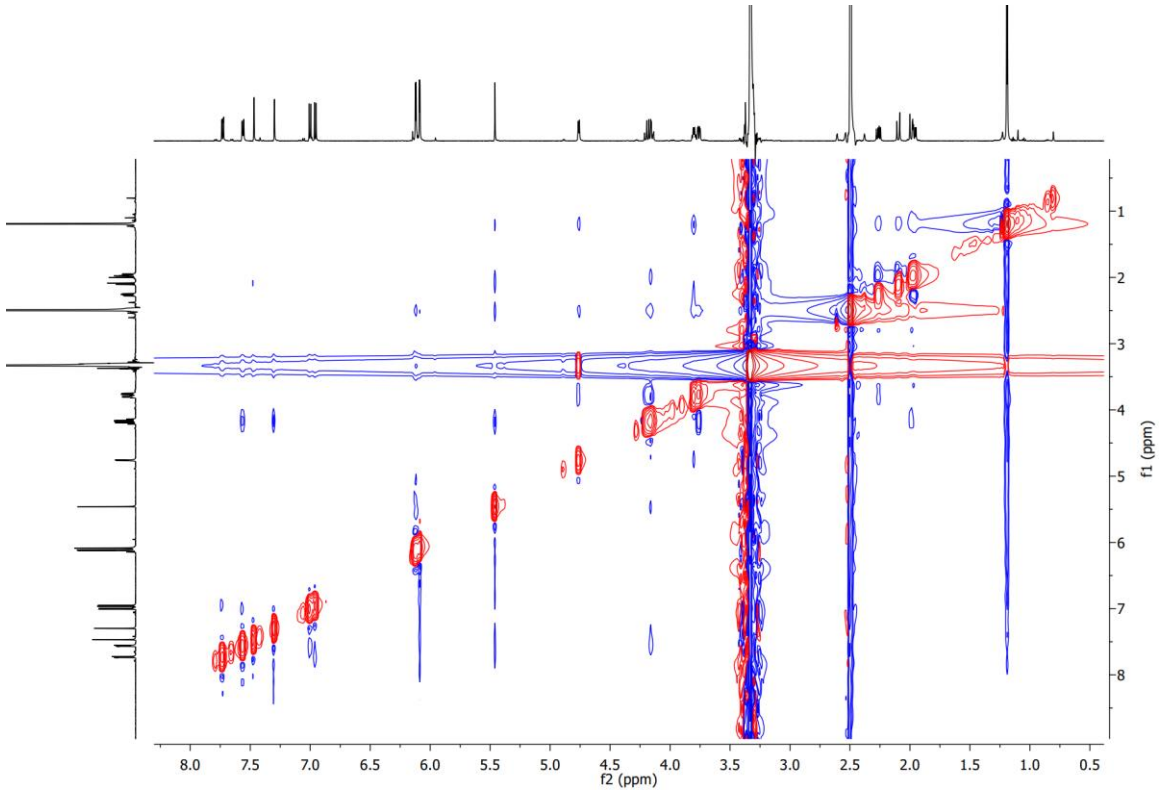

Figure S6.8. ROESY spectrum (600 MHz, DMSO-d_6) of compound **3**

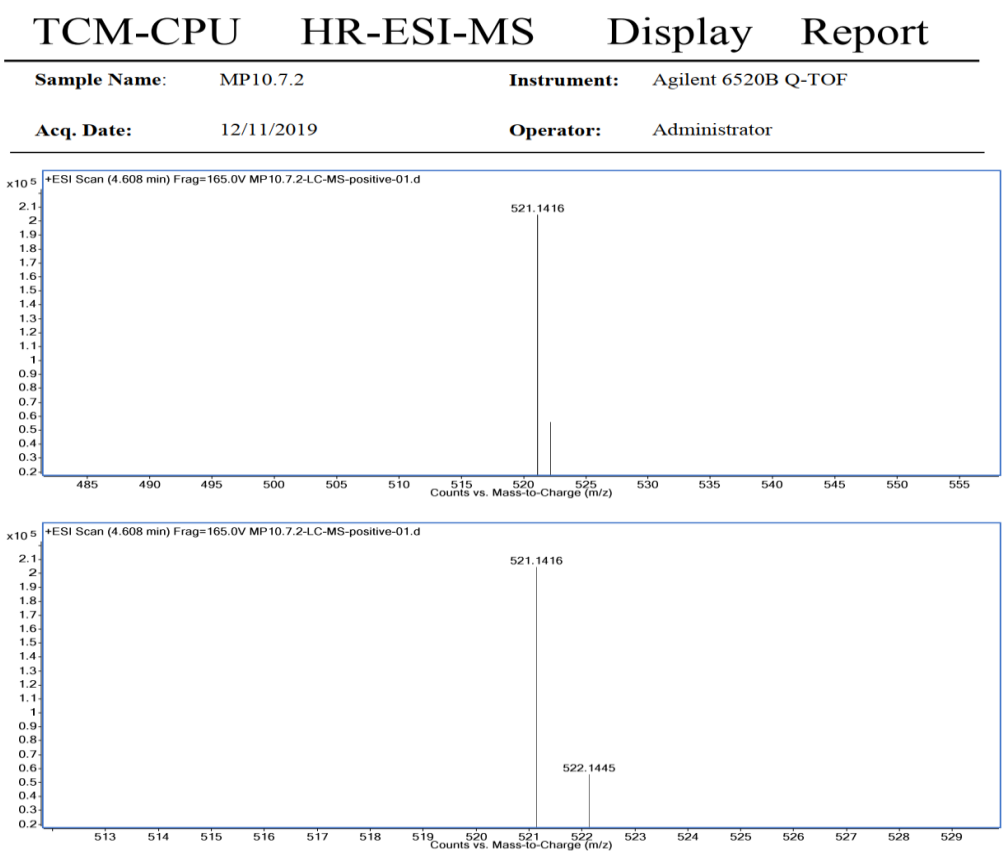

Figure S6.9. HRESIMS spectrum of compound **3**

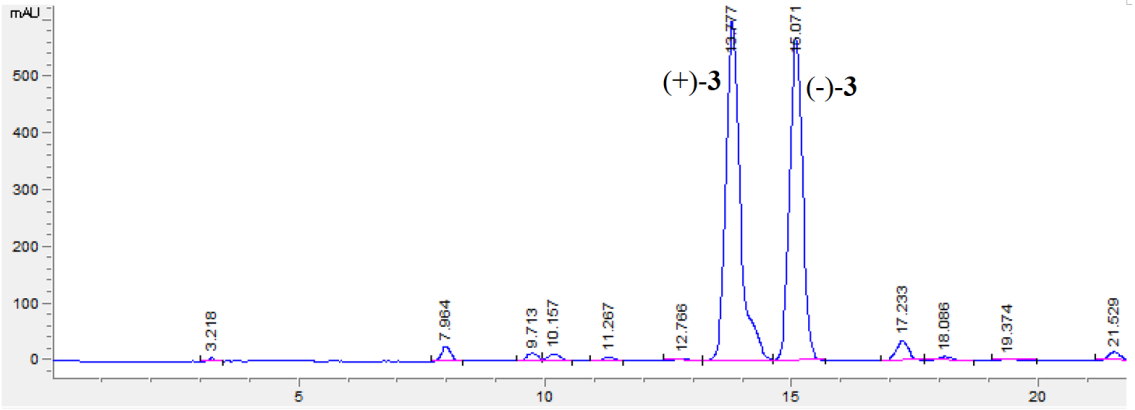

Figure S6.10. Chiral HPLC chromatogram of compound **3**